Band structure and absorption coefficient in GaN/AlGaN quantum wires*

Yao Wen-Jie(姚文杰), Yu Zhong-Yuan(俞重远)†, and Liu Yu-Min(刘玉敏)

Key Laboratory of Information Photonics and Optical Communications, Ministry of Education, Beijing University of Posts and Telecommunications, Beijing 100876, *China*

(Received 28 September 2009; revised manuscript received 5 January 2010)

The band structures of rectangular GaN/AlGaN quantum wires are modeled by using a parabolic effective-mass theory. The absorption coefficients are calculated in a contact-density matrix approach based on the band structure. The results obtained indicate that the peak absorption coefficients augment with the increase of the injected carrier density, and the optical gain caused by interband transition is polarization anisotropic. For the photon energy near 1.55 eV, we can obtain relatively large peak gain. The calculations support the previous results published in the recent literature.

Keywords: absorption coefficient, gain, polarization anisotropic, quantum wires
PACC: 7110, 7320D, 7115, 7865

1. Introduction

Nanostructure semiconductor materials such as quantum wires (QWRs)[1,2] and quantum dots (QDs) have been hotpoints of experimental and theoretical research in the recent years. With the increase of the confinement degree, low-dimensional semiconductor materials have shown advanced applications in optoelectronic and microelectronic devices, such as, light emission diodes, solar cells, semiconductor laser[3,4] and optical amplifiers.[5] Also, low-dimensional quantum structures can be used to design left-handed materials[6] and generate negative refraction[7] in anisotropic waveguides. The photoluminescence spectra have been investigated experimentally for intraband transition in quantum wires.[8] Band structures and intersubband absorptions in V-groove quantum wires have been researched by Crnjanski and Gvozdic[1] and Takahashi *et al.*[2] But the interband absorption and the effect of polarization on optical absorption are investigated very little.

In this paper, we investigate the band structures, absorption coefficients (or gain coefficients) for interband transition and intersubband transition in the rectangular GaAs/$Ga_{0.6}Al_{0.4}As$ quantum wires. For simplicity, size fluctuation is not included, which should be considered for practical QWRs. But the effect of polarization on absorption coefficient is considered. To understand the band structure of the one-dimensional electron (or hole) system in a quantum wire, the calculation of energy eigenvalues and eigenvectors is very important. Approaches to solving one-dimensional Schrödinger equations are well developed. However the added degree of quantum confinement existing in lower-dimensional systems, such as one-dimensional quantum wires and zero-dimensional quantum dots, produces a highly increased complexity in the Schrödinger equations which need to be solved with the finite element method (FEM)[9−11] or plane wave expansions[12] to obtain accurate solutions.

2. Theory

Here we introduce a simple, almost analytical technique for approximating the solutions in rectangular cross-section quantum wires. The band structures are modeled with a parabolic effective-mass model without valance-band mixing. Valance-band–mixing has only perturbation effect on the band structure and thus does not have a significant qualitative effect on absorption and gain spectrum, because the heavy-hole and light-hole subbands are separated in energy. For further research, the piezoelectric effect and the strain effect on band edge should be considered, which is not investigated in this paper. The

*Project supported by the National High Technology Research and Development Program of China (Grant No. 2009AA03Z405), and the National Natural Science Foundation of China (Grant Nos. 60908028, 60971068 and 60644004).
†Corresponding author. E-mail: yuzhongyuan30@gmail.com
© 2010 Chinese Physical Society and IOP Publishing Ltd

two-dimensional time-independent Schrödinger equation in the effective-mass approximation is given by

$$-\frac{\hbar^2}{2m^*}\left(\frac{\partial^2}{\partial x^2}+\frac{\partial^2}{\partial y^2}\right)\psi(x,y)+V(x,y)\psi(x,y) = E\psi(x,y), \quad (1)$$

where m^* represents the effective mass of carrier and the potential function is just space-dependent.

If $V(x,y)$ is the general potential energy, there exists no easy way to solve this equation, but great simplification occurs for a rectangular quantum wire as it can be written as a sum of two independent potentials $V(x)$ and $V(y)$ and a perturbation $\Delta V(x,\ y)$, i.e.

$$V_{2\mathrm{D}}(x,y)=V_{1\mathrm{D}}(x)+V_{1\mathrm{D}}(y)+\Delta V(x,y). \quad (2)$$

A sketch of the perturbation for rectangular QWRs is presented in Fig. 1. Then the unperturbed equation can be separated into the following two one-dimensional equations:

$$-\frac{\hbar^2}{2m^*}\frac{\partial^2}{\partial x^2}\phi(x)+V(x)\phi(x)=E_x^0\phi(x), \quad (3)$$

$$-\frac{\hbar^2}{2m^*}\frac{\partial^2}{\partial y^2}\phi(y)+V(y)\phi(y)=E_y^0\phi(y). \quad (4)$$

The final eigenenergy E is obtained from the unperturbed eigenenergies, E_x^0 and E_y^0, by adding the first-order perturbation $\Delta E = \langle\psi|\Delta V(x,\ y)|\psi\rangle$, i.e. $E=E_x^0+E_y^0+\Delta E$.

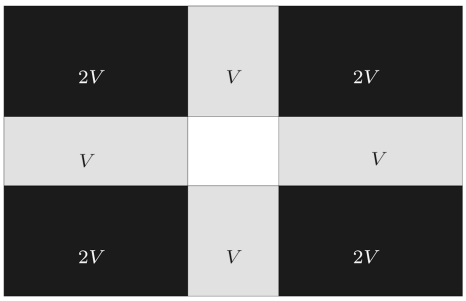


Fig. 1. Confining potential used for a rectangular QWR.

In the present calculation, we consider the intersubband transition and the interband transition separately. The transition matrix element can be expressed as follows:

$$H'_{ba} = \langle b\,|H'|\,a\rangle = \langle u_b\,|H'|\,u_a\rangle_{\mathrm{cell}}\,\langle\psi_b|\psi_a\rangle + \langle u_b|u_a\rangle_{\mathrm{cell}}\,\langle\psi_b\,|H'|\,\psi_a\rangle\,, \quad (5)$$

where H' describes the interaction between the material and the optical field; u_a and u_b are the periodic parts of Bloch functions for a subband energy and b subband energy; ψ_a and ψ_b are the real wave functions. Using the orthonormal conditions, we have

$$\langle\psi_b|\psi_a\rangle=0,\quad \langle u_b|u_a\rangle_{\mathrm{cell}}=1,\quad H'_{ba}=\langle\psi_b\,|H'|\,\psi_a\rangle \quad (6)$$

for intersubband transition, and

$$\langle u_b|u_a\rangle_{\mathrm{cell}}=0,\quad H'_{ba}=\langle u_b\,|H'|\,u_a\rangle_{\mathrm{cell}}\,\langle\psi_b|\psi_a\rangle \quad (7)$$

for interband transition. Then the optical absorption coefficient $\alpha(\omega)$ for intersubband transition and the gain coefficient $g(\omega)$ for interband transition can be expressed, respectively, as

$$\begin{aligned}\alpha(\omega) &= \frac{\omega N_{\mathrm{D}}}{n_r C\varepsilon_0}\sum_{\boldsymbol{k}_a,\boldsymbol{k}_b}|\hat{e}\cdot\mu_{ba}|^2\delta(E_b-E_a-\hbar\omega)\\ &\quad\times(f_c(E^a)-f_c(E^b)),\\ g(\omega) &= C_0\frac{2}{V}\sum_{\vec{k}_a}\sum_{\boldsymbol{k}_b}|\hat{e}\cdot P_{ba}|^2\delta\left(E_g+E_a^{\mathrm{e}}-E_b^{\mathrm{h}}-\hbar\omega\right)\\ &\quad\times\left(f_a^{\mathrm{e}}-f_b^{\mathrm{h}}\right),\\ C_0 &= \frac{\pi e^2}{n_{\mathrm{r}}C\varepsilon_0 m_0^2\omega},\end{aligned} \quad (8)$$

where ω is the transition energy, N_{D} is the injected carrier density, C is the speed of light, n_{r} is the refractive index, ε is the permittivity of the free space, m is the free electron mass, V is the effective volume of the quantum wire, $\hat{e}$ denotes the unit vector in the direction of optical electric field, μ_{ba} is the dipole moment matrix element for electron between a subband and b subband multiplied by the overlap of the wave functions, E_a and E_b, respectively, denote the a subband energy and b subband energy in conductor band, f_c is the electron Fermi function,P_{ba} is the optical momentum matrix element between a electron subband and b hole subband multiplied by the overlap of the wave functions, E_{g} is the band gap. E_a^{e} and E_b^{h}, respectively, denote the a electron subband energy and b hole subband energy, and f_a^{e} and f_b^{h} are, respectively, the electron and the hole Fermi functions. The absorption coefficient α is opposite to the optical gain $g(\omega)$ in sign, i.e. $\alpha(\omega)=-g(\omega)$. To obtain the optical absorption spectrum, we first need to calculate the electron and hole Fermi levels, $E_{\mathrm{F}}^{\mathrm{e}}$ and $E_{\mathrm{F}}^{\mathrm{h}}$, which depend on the injected carrier density.

3. Results and discussion

In the calculation, the following parameters are used:[13] for electron, $m_{\mathrm{W}}=0.0665m_0$, $m_{\mathrm{B}}=0.0858m_0$, and $V=276$ meV; for heavy hole, $m_{\mathrm{W}}=0.3774m_0$, $m_{\mathrm{B}}=0.3865m_0$, and $V=184$ meV; for

light hole, $m_{\rm W} = 0.0905m_0$, $m_{\rm B} = 0.1107m_0$, and $V = 184$ meV; the band gap for GaAs is 1.424 eV. Calculations are made for different values of base width L_x, ranging from 4 to 20 nm, with the ratio between base width L_x and height L_y kept constant, i.e. $L_x/L_y = 1:1$. The results are presented in Fig. 2(a). The electron energy decreases, as the wire width increases. The minimum of electron energy is smaller than the confining potential for $L_x \geq 4$ nm, which means that this state is bound. But when $L_x < 4$ nm, the minimum of electron energy is larger than the confining potential, which means that there exists no bound state. It is conflict with the theoretical prediction in that a quantum wire has always at least one bound state, and so it could be meant that our model is not suitable for very narrow wires with the linear dimensions less than 4 nm. In Fig. 2(b), it can be seen that the heavy hole energy level is smaller than the corresponding light hole energy level in amplitude.

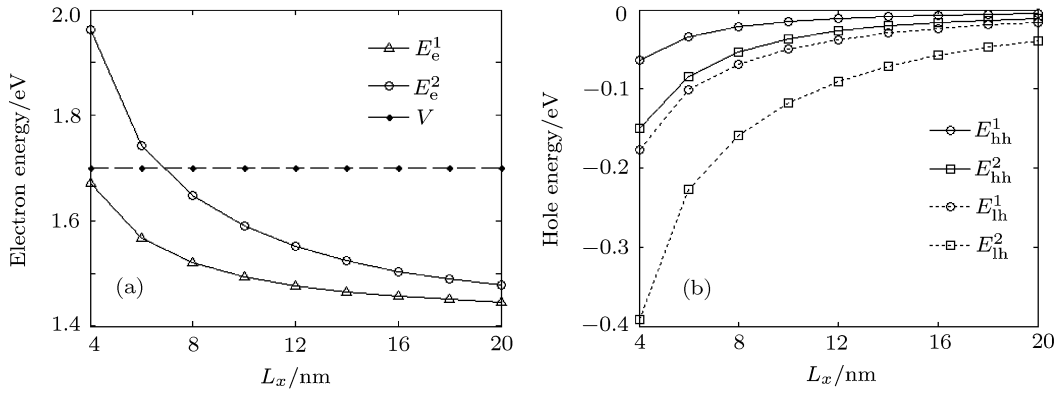


Fig. 2. Energies of lowest two subbands against L_x with $L_x/L_y = 1:1$ (a), for the conduction band and the valance band (heavy hole and light hole) (b).

The densities of states (DOSs) for the electrons in the conduction band and for the holes in the valance band are calculated, after the energy band structures have been obtained. Figure 3 shows the DOSs for the electrons and the holes versus energy with $L_x = L_y = 10$ nm. The peaks of DOS correspond to the energy levels. Between two adjacent energy levels, the DOS decreases with the energy increasing. For the energy less than the energy of lowest subband, the DOS is zero. It means there to be no state occupied by electrons (or holes). In Fig. 3, it can be seen that the electron DOS is smaller than the heavy hole DOS. As a result, the electron distribution is more widespread in energy than the heavy hole distribution.

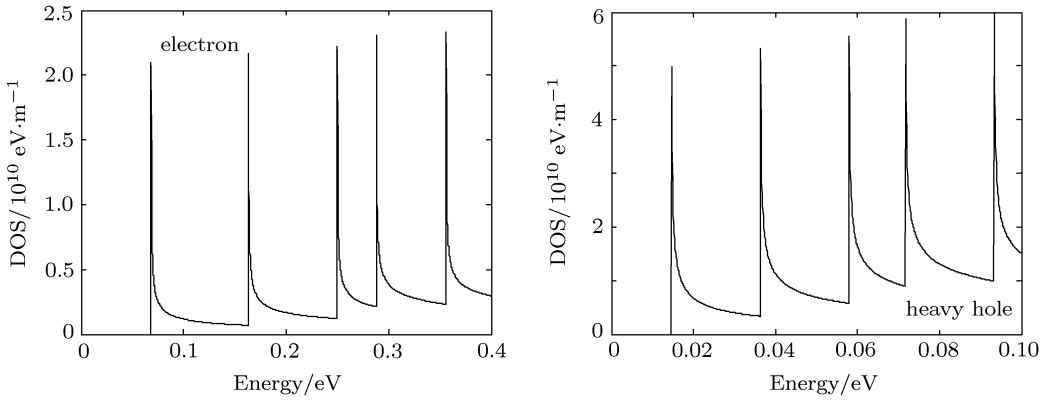


Fig. 3. DOSs for electron and hole of QWR structures without size fluctuation, for $L_x = L_y = 10$ nm.

To understand the optical characteristic of quantum wire, we mainly investigate the intersubband absorption and the interband gain spectrum. In Fig. 4, the absorption coefficient for intersubband bound-to-bound transition in the conduction band is shown as a function of the photon energy. When the scattering relaxation between electron and photon is included, the delta function may be replaced by a Lorentz function with linewidth $\Gamma = 2$ meV, and given as

$$\delta(E_b - E_a - \hbar\omega) = \frac{\Gamma/(2\pi)}{(E_b - E_a - \hbar\omega)^2 + (\Gamma/2)^2}, \quad (9)$$

where Γ is the broadening parameter due to the electron-phonon interaction, and collisions among electrons, etc.

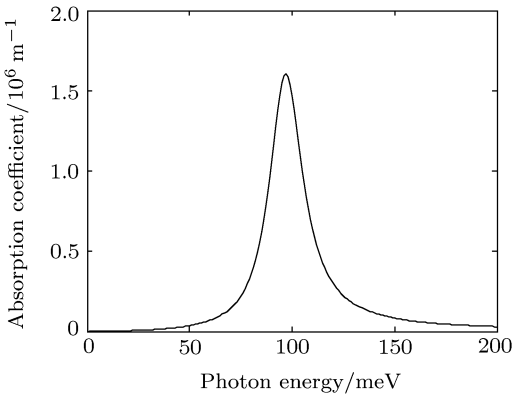


Fig. 4. Absorption coefficient for intersubband bound-to-bound transition in the conduction, with $L_x = L_y =$ 10 nm, the injected carrier densities, N_e and N_h, both being 1.0×10^{24} m^{-3}.

In Fig. 4, it can be seen that there is just one peak on the curve. This is because at this injected carrier density, only the first subband is occupied and other subband populations are indeed small. For intersubband transition, the absorption spectra of transverse electric (TE) polarization (along the y direction) and transverse magnetic (TM) polarization (along the x direction) are the same for QWRs with symmetric structures when the incident light propagates along the x direction.

From the numerical results obtained in the previous section we could evaluate the interband transition performance for QWR structures. Figure 5 shows the interband gain spectra against photon energy. In Fig. 5(a), it can be seen that there are two peaks on each curve. That is because under these injected carrier densities, interband transitions occur mainly between the electrons and the heavy holes (or light holes). As injected carrier density increases, the gain coefficient gradually becomes bigger. When the injected carrier density is great enough, the electron (or heavy/light hole) does not mainly locate in the ground state. Then there will be more than two peaks on the curve for the gain spectra caused by interband transition. In Fig. 5(b), we can find that the gain spectra for TE polarization and TM polarization are different from each other. For the TM polarization, the gain caused by the transition between electron and heavy hole is much larger than that caused by the transition between electron and light hole. But for the TM polarization, they are almost the same. Here the anisotropy of the optical gain for QWRs is proved. We can also find that the larger optical gains are obtained for the photon energy near 1.55 eV.

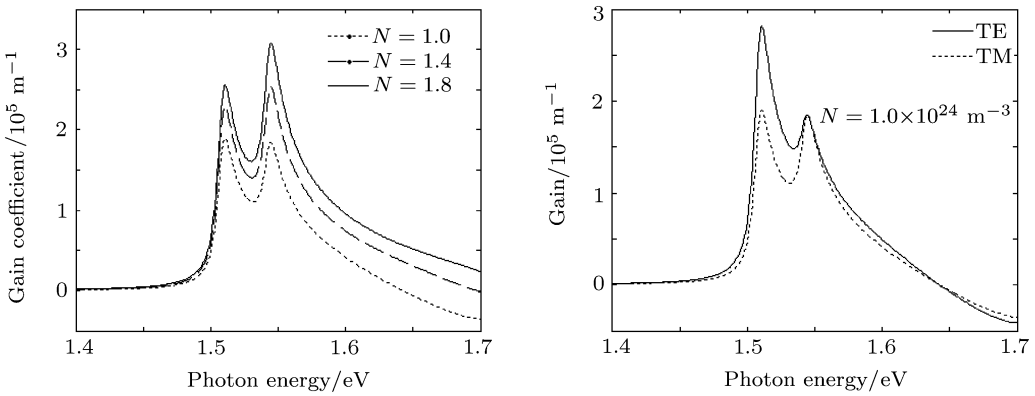


Fig. 5. Gain coefficients against photon energy for interband transition, showing (a) TM polarization with the injected carrier density (N) varying from 1.0×10^{24} m^{-3} to 1.8×10^{24} m^{-3}, and (b) TE polarization and TM polarization for $N = 1.0\times10^{24}$ m^{-3}.

4. Conclusions

We investigate the energy band structure of QWRs by the parabolic effective-mass theory, which is accurate for the QWRs with diameters larger than 4 nm. For further research, the effects of strain and piezoelectric potential should be taken into account, also the Schrödinger equation should be solved by multi-band theory, which are beyond the scope of our present work. The results obtained indicate that the absorptions caused by intersubband transition are the same for TE polarization and TM polarization, but the absorption and the gain spectrum caused by interband transition are anisotropic. It provides the theoretical guidance for the design of devices made of QWRs. Due to the effects of strain and piezoelectric polarization on conduction band and valance band edge, the band structures will be modified in the lattice-mismatch materials.[14−16] For further research, the strain and the polarization should be taken into account to investigate the optical properties in QWRs.

References

[1] Crnjanski J V and Gvozdic D M 2007 *J. Appl. Phys.* **101** 013104

[2] Takahashi Y, Hayamizu Y, Itoh H, Yoshita M and Akiyama H 2005 *Appl. Phys. Lett.* **87** 223119

[3] Liu Y M, Yu Z Y and Huang Y Z 2007 *J. Univ. Sci. Technol.* B **14** 477

[4] Liu Y M, Yu Z Y and Ren X M 2007 *Chin. Phys. Lett.* **25** 1850

[5] Alizon R, Hadass D, Mikhelashvili V, Einsenstein G, Schwertberger R, Somers A, Reithmaier J P, Forchel A, Calligaro M, Bansropun S and Krakowski M 2004 *Electron. Lett.* **40** 760

[6] Ginzburg P and Orenstein M 2008 *J. Appl. Phys.* **103** 083105

[7] Plumridge J R, Steed R J and Phillips C C 2008 *Phys. Rev.* B **77** 205428

[8] Moret N, Oberli D Y, Dwir B, Rudra A, Gallo P and Kapon E 2008 *Appl. Phys. Lett.* **93** 172107

[9] Cusack M A, Briddon P R and Jaros M 1996 *Phys. Rev.* B **54** R2300

[10] Liu Y M, Yu Z Y, Ren X M and Xu Z H 2008 *Chin. Phys.* B **17** 3471

[11] Liu Y M, Yu Z Y and Ren X M 2009 *Chin. Phys.* B **18** 0881

[12] Gershoni D, Temkin H, Dolan G J, Dunsmuir J, Chu S N G and Panish M B 1998 *Appl. Phys. Lett.* **53** 995

[13] Califano M and Harrison P 1999 *J. Appl. Phys.* **86** 5054

[14] Yao W J, Yu Z Y, Liu Y M and Lu P F 2009 *Acta Phys. Sin.* **58** 1185 (in Chinese)

[15] Schliwa A, Winkelnkemper M and Bimberg 2007 *Phys. Rev.* B **76** 205324

[16] Xiang H J, Wei S H, Silva J L F D and Li J B 2008 *Phys. Rev.* B **78** 193301